Journal of Polymer Research (2021) 28: 288
https://doi.org/10.1007/s10965-021-02645-4

ORIGINAL PAPER

Self-assembled drug-polymer micelles with NO precursor loaded for synergistic cancer therapy

Yuanbao Jin[1] · Liying Wang[1] · Yumeng Liu[1] · Xiaomei Liu[1] · Tian Zhong[1,2]

Received: 3 January 2021 / Accepted: 30 June 2021 / Published online: 9 July 2021

Abstract

Self-assembled drug-polymer micelles are attractive candidates for drug delivery. In this study, amphiphilic floxuridine (FdU)-poly ε-caprolactone (PCL) conjugates containing ester bond were synthesized and self-assembled with phenylsulfonyl furoxan (PSF) to form drug-loading micelles. The micelles had an average size of 91.2 nm and a critical micelle concentration (CMC) of 8.56 μg mL^{-1}. The Micelles were stable in physiological environment, but would decompose under intracellular conditions, releasing chemotherapeutic drug FdU and NO precursor PSF in cancer cells. Intracellular glutathione (GSH) triggered NO release from the PSF, with which the FdU inhibited cancer cells synergistically. In vitro cell and in vivo small animal experiments demonstrated that the Micelles could accumulate in the tumor and be internalized by cancer cells. The micelles inhibited the cancer cell proliferation by releasing FdU and NO. The NO acted as an MDR reversal agent and hence increased the intracellular FdU concentration, through which synergistic therapy was achieved. This drug-polymer conjugate-based micelles had high therapeutic efficacy for cancer with low side effects, providing a new approach to cancer chemotherapy.

Keywords Drug-polymer conjugate · Self-assembled micelle · Nitric oxide · Co-delivery · Cancer therapy

Introduction

Nitric oxide (NO) is a short-lived free radical that has been receiving intensive attention during the past decades. As an important messenger molecule, NO participates in a variety of physiological processes [1–4], including immune response to infections [5], angiogenesis [6], platelet aggregation and adhesion [7], wound healing [8], sleep control and regulation [9], etc. It has been proved that NO is able to inhibit cancer progression [10–12]. Exogenous delivery of NO has become a promising therapeutic method to fight against cancer. People have developed various NO delivery platforms for cancer therapy, among which the drug delivery systems releasing both NO and chemotherapeutic drug are intriguing candidates of anticancer agents [13–16]. Due to the extremely active nature of NO, it is almost impossible to load NO directly in a carrier. Instead, NO precursor molecules are frequently used as NO reservoirs, which were integrated into appropriate carriers to form NO releasing systems.

NO precursors such as N-diazeniumdiolates, S-nitrosothiols, organic nitrates, have been intensively studied for biomedical purposes [17–19]. Phenylsulfonyl furoxan (PSF) is a NO precursor molecule that releases NO in response to glutathione (GSH) [20]. Similar to most NO precursors, PSF is a hydrophobic molecule and needs a carrier to deliver itself in order to achieve optimal efficacy. Amphiphilic polymeric micelles [21, 22] are favored materials for loading PSF, since their hydrophobic core is compatible with the PSF molecules. Alternatively, micelles from amphiphilic polymer-drug conjugates [23–25] may be used for loading NO precursors. The polymer-drug micelles have an edge over polymeric micelles, as the polymer-drug micelles themselves have therapeutic efficacy. In addition, the drug loading content of these micelles is higher compared with the polymeric micelles.

Usually, polymer-drug conjugates deliver only one drug. In practical applications, co-delivery of two or even more drugs is sometimes required to strengthen the therapeutic

✉ Tian Zhong
zhongtiancc@foxmail.com

[1] School of Pharmacy and Food Science, Zhuhai College of Jilin University, Zhuhai, Guangdong, China

[2] Faculty of Medicine, Macau University of Science and Technology, Avenida Wai Long, Taipa, Macau, China

effects. Loading an additional drug in polymer-drug micelles for dual drug delivery is rarely reported, which is especially important for NO-assisted chemotherapy. In the present work, we report a new type of micelles assembled from amphiphilic drug-polymer conjugates, which are capable of co-delivering chemotherapeutic drug and NO to treat cancer. As illustrated in Fig. 1, hydrophobic poly ε-caprolactone (PCL) molecular chains were reacted with hydrophilic drug floxuridine (FdU) via esterification to form the amphiphilic FdU-PCL conjugates, which were able to self-assemble into micelles. In the meantime, the hydrophobic PSF was entrapped in the hydrophobic core of the micelles, producing a system for stimuli-responsive delivery of both chemotherapeutic drug and NO. Once the Micelles were internalized by the cancer cells, the intracellular environment stimulates the decomposition of the Micelles, leading to the release of FdU and PSF.

Experimental section

Materials

Floxuridine (FdU, 98%) was provided by Adams. Poly ε-caprolactone (PCL, $M_n = 2000$) was purchased from Alfa Aesar. 4-(Dimethylamino)pyridine (DMAP, 99%) and N,N′-dicyclohexylcarbodiimide (DCC, 99%) were purchase from J&K. Dulbecco's modified Eagle's medium (DMEM), fetal bovine serum (FBS) and 3-(4,5-dimethyl-thiazol-2-yl)-2,5-diphenyl tetrazolium bromide (MTT) were purchased from Sigma. PSF was synthesized according to the protocols described in a previous work [1]. All other chemicals and solvents were provided by Sinopharm Chemical Reagent Co., Ltd and used as received without further purification (analytically pure). Millipore water was used in all the experiments.

Synthesis of FdU-PCL conjugates

0.5 mmol of PCL and 0.6 mmol of DCC were dissolved in 0.7 mL of anhydrous DMF, which was cooled to 0 °C and was stirred for 30 min. 1.5 mmol of FdU, 0.05 mmol of DMAP, 0.5 mmol of triethylamine (TEA) and 8 mL of dimethyl formamide (DMF) were mixed together to obtain a solution, into which the above mixture was added dropwise and stirred at room temperature for 48 h. The resultant mixture was filtered and vacuum-evaporated to give a light yellow solid, i.e., FdU-PCL conjugates. ^{13}C NMR (400 MHz, DMSO-d_6) δ (ppm): 157.11, 149.12, 143.36, 141.65, 139.27, 124.73, 101.96, 85.72, 77.1, 70.49, 64.67, 62.50, 40.98, 33.47, 29.02, 25.57. ESI–MS m/z ($M + H^+$): calcd 2241.6430, found 2241.6389 ($M + H^+$).

Preparation of PSF-loading Micelles

0.2 g of FdU-PCL conjugates was dissolved in 15 mL of DMSO, where an appropriate amount of PSF was then added [15], and the mixture was stirred at room temperature for 1 h. Subsequently, the mixture was added dropwise to 100 mL of water, which was stirred for 3 h. The resultant solution was dialyzed against water in a dialysis bag (MWCO = 2000 Da) for 36 h to produce the PSF-loading Micelles.

Determination of PSF loading

The loading content (LC) and loading efficiency (LE) of PSF were calculated respectively by the following equations:

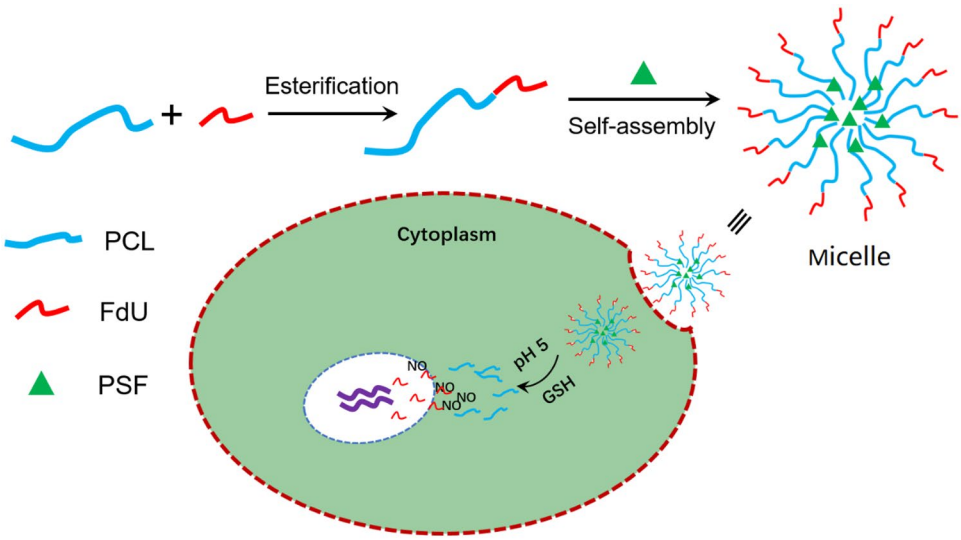

Fig. 1 Schematic presentation of synthesis, self-assembly, cell uptake, and intracellular drug delivery of the Micelles

$$LC_{PSF} = \frac{weight\ of\ loaded\ PSF}{weight\ of\ Micelles} \times 100\% \quad (1)$$

$$LE_{PSF} = \frac{weight\ of\ loaded\ PSF}{weight\ of\ PSF\ in\ feed} \times 100\% \quad (2)$$

The weight of PSF was determined by measuring the amount of S element with a Vario EL cube elemental analyzer (Elementar, Germany).

Characterization

^{1}H and ^{13}C nuclear magnetic resonance spectroscopy was conducted on a Mercury Plus-400 spectrometer at 400 MHz (Varian, US). Sample morphology was observed using a JEM-2100 transmission electron microscope (TEM, JEOL, Japan). Size distribution of samples were determined by a Nano ZS90 particle size and zeta potential analyzer (Malvern, UK) based on dynamic light scattering (DLS) at a scattering angle of 90°. The molecular weight of the Micelles and the cleavage products was measured on a 1260 Infinity series gel permeation chromatography (GPC, Agilent, US) using 10 μm PLgel 600 × 7.5 mm column.

Measurement of FdU release

The release of FdU from the Micelles was measured under simulated physiological conditions. Typically, freeze-dried Micelles were dissolved in phosphate buffered saline (PBS) buffers with pH 7.4 and pH 5, respectively. 4 mL of the Micelles solution (1 mg mL^{-1}) was transferred into a dialysis tube with a MWCO of 1000 Da, which was then immersed in a beaker filled with 46 mL of PBS buffer under gentle stirring at 37 °C. At predetermined time points, 2 mL of the external buffer was replaced by 2 mL of fresh medium. Then the withdrawn external buffer was measured by a UV–vis spectrometer to determine the amount of FdU. The UV absorption spectrum of FdU is shown in Fig. S1, based on which the FdU concentration was measured. The measurements were conducted in triplicate.

Measurement of NO release

Quantitative analysis of NO released from the Micelles under different conditions was conducted by a TBR 4100/1025 free radical analyzer equipped with an ISO-NOP sensor (WPI Ltd., US). The detailed NO detection protocols have been described in our previous work [2].

Cell culture

Human Cervical Carcinoma (HeLa) cells were purchased from Institute of Biochemistry and Cell Biology, Chinese Academy of Science. The cells were cultured in Dulbecco's Modified Eagle's medium (DMEM) supplemented with 10 wt% FBS, 100 IU/mL penicillin and 100 μg mL^{-1} streptomycin in a humidified incubator with 5 vol% carbon dioxide at 37 °C. The medium was refreshed every 2 or 3 days according to cell density.

Cell imaging

Around 0.5 mL of HeLa cell suspension was added to an eight-well Lab-Tek II chamber slide (Nalge Nunc, Napevillem, IL), followed by removing the culture medium and adding 0.5 mL of 20 μg mL^{-1} Micelles as well as 1.2 μg of Cu-2-{2-chloro-6-hydroxy-5-[(2-methyl-quinolin-8-ylamino)-methyl]-3-oxo-3H-xanthen-9-yl}-benzoic acid (CuFL). The cells were then incubated for 2 h for uptake of the Micelles. At different time points, the medium was aspirated from the wells, and the cells were rinsed with fresh culture medium for three times. The fluorescence emission from the cells was observed by a confocal laser scanning microscope (Zeiss LSM 710, Germany).

MTT assay

The cultured HeLa cells were seeded in 96-well culture plates at a density of ~ 5500 cells/well and incubated at 37 °C for 24 h. The culture medium was then replaced by a fresh medium containing FdU, FdU/PSF mixture, Micelles and blank micelles (FdU-PCL micelles without PSF loaded) at different concentrations. After incubation for another 24 h, the culture plates were rinsed with a PBS buffer to remove unattached cells and the remaining cells were treated with 5 mg mL^{-1} MTT stock solution in PBS for 4 h. The medium containing unreacted MTT was carefully removed. The obtained formazan was dissolved in DMSO, and the absorbance of individual wells was recorded at 570 nm using a Multiskan MK3 Enzyme-labeled Instrument (Thermo Scientific, US). The cell viability was determined by the following equation:

Cell viability % = Absorbance of test cells/Absorbance of control cells × 100% (1).

Western blot analysis

HeLa cells were cultured in 6-well plates with 1.5 mL of complete DMEM at a density of 6.2×10^5 cells/well for 24 h. Then the cells were incubated with FdU, FdU/PSF mixture, Micelles and blank micelles respectively at the same equivalent FdU concentration of 10 μg mL^{-1} for 12 h. Untreated HeLa cells were used as a control. Afterwards, the cells were washed with PBS buffer twice and lysed in an ice-cold lysis buffer. The cell lysates were separated by gel electrophoresis

using 12% sodium dodecyl sulfate–polyacrylamide gels (SDS-PAGE). The protein bands were transferred onto polyvinylidene fluoride (PVDF) membranes, which were incubated in 5% skimmed milk dissolved in Tris buffered saline containing 0.05% Tween-20 (TBST) at 37 °C. The membranes were reacted with relevant primary antibodies against β-actin (loading control) and P-gp (dilution of 1:1000) at 4 °C. After washing with TBST, the membranes were incubated with horseradish peroxidase (HRP)-labeled anti-rabbit immunoglobulin-G (dilution of 1:5000) at room temperature. The protein bands were analyzed using a ChemiDoc MP Imaging System (Bio-Rad, US).

Animal tumor model

Eight weeks old female BALB/c mice (~ 20 g) purchased from Shanghai Institute of Zoology, Chinese Academy of Science were adopted to construct a mouse xenograft model. All the in vivo experiments were performed according to approved protocols by the Animal Ethics Committee of Shanghai Jiao Tong University. The mice were randomly divided into four groups. The cells were washed twice by PBS buffer and were suspended in sterile normal saline. Around 1.8×10^6 HeLa cells were subcutaneously injected in the flank region of the mice. Till the inoculated tumors grew to a volume of ~ 120 mm^3, the mice were tail vein injected with PBS (100 μL, control), FdU, FdU/, Micelles (100 μL, 1 mg FdU/kg) every other day for a total of 12 days. The tumor volumes and body weights of each group were measured every other day.

Biodistribution

The tumor-bearing mice were treated with tail vein injection of FdU and the Micelles (100 μL, 1 mg FdU/kg). The mice were sacrificed at 6 h and 24 h post injection. The lung, stomach, liver, spleen, kidney and tumor were harvested, blotted with paper towel and weighed. The tissue samples were rinsed in saline, frozen in liquid nitrogen and homogenized. The FdU and the Micelles were extracted from the

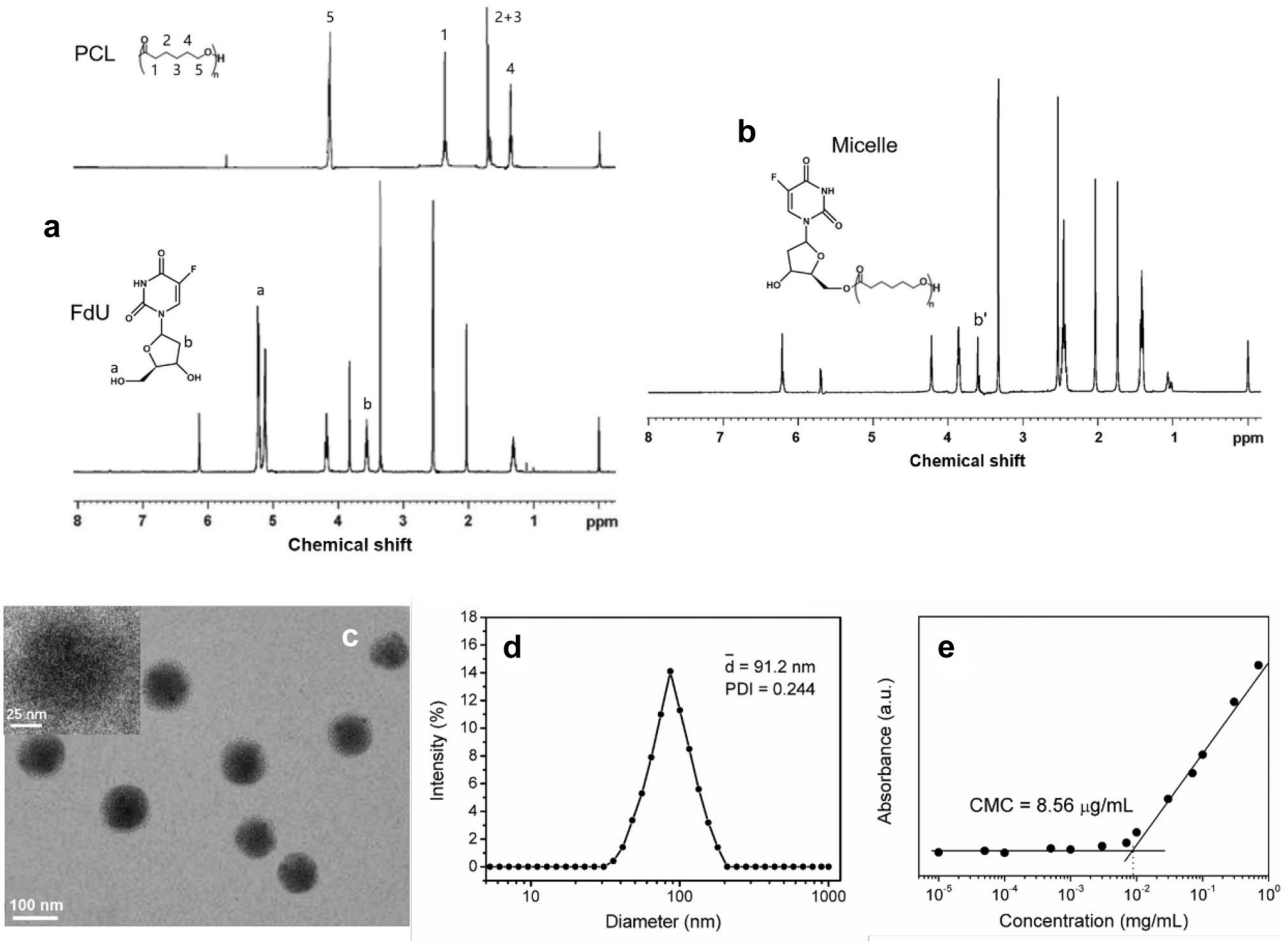

Fig. 2 (**a**) ^{1}H NMR spectra of PCL and FdU. (**b**) ^{1}H NMR spectrum of the FdU-PCL conjugates. (**c**) TEM micrograph of the Micelles; the inset shows a micrograph of a typical Micelle. (**d**) Size distribution of the Micelles based on DLS. (**e**) Plots of absorbance intensity of DPH against Micelles concentration at room temperature. The CMC was determined by the crossover of the fitting lines

homogenates using 2 mL of dichloromethane/methanol (4:1, v/v). The organic phases were collected and dried, and were then dissolved in acetonitrile for analysis. The resultant samples were measured by a Water ACQUITY UPLC system (Waters, US).

Statistical analysis

Student's t-test was used to evaluate the statistical significance of differences between groups. Values were represented as mean ± standard deviation and the data were considered as statistically significant at $^{*}P < 0.05$ or $^{**}P < 0.01$.

Results and discussion

Chemical composition and physical properties

^{1}H nuclear magnetic resonance (NMR) spectroscopy was used to characterize the molecular structure of the FdU-PCL conjugates. Figure 2a, b show the characteristic resonance peaks of PCL, FdU and the conjugates. It is clear that the peak at 5.21 ppm (a) ascribed to the hydroxyl proton of FdU was absent in the spectrum of the FdU-PCL conjugates. Besides, the peak at 3.54 ppm (b) corresponding to $-CH_2-$ of FdU shifted slightly to lower field when FdU was reacted with PCL. The ^{1}H NMR results confirmed the esterification reaction between FdU and PCL.

The self-assembled FdU-PCL micelles (named as Micelles) were observed by transmission electron microscopy (TEM), and the TEM micrographs are shown in Fig. 2c. The Micelles showed spherical profiles with an average diameter of below 100 nm. The TEM micrograph with higher magnification (the inset) indicates the morphology of a single Micelle, which was similar to that of the polymer-drug micelles reported in a previous work [24]. Hydrodynamic size and size distribution of the Micelles were determined based on dynamic light scattering (DLS). In Fig. 2d, the size distribution profile demonstrates an average diameter of 91.2 nm and a polydispersity index (PDI) of 0.205. The critical micelle concentration (CMC) of the Micelles was obtained using 1,6-Diphenyl-1,3,5-hexatriene (DPH) as a hydrophobic ultraviolet (UV) probe. The absorbance of DPH versus Micelles concentration at room temperature is shown in Fig. 2e. With the increase of concentration, the UV absorbance changed slightly until the concentration exceeded a critical value. The CMC was determined by the crossover of the two fitting lines, which turned out to be 8.56 μg mL^{-1}, in the same order of magnitude as that of reported polymer-drug micelles [24]. The loading content (LC) and loading efficiency (LE) of PSF were 6.7 wt% and 30.9 wt%, respectively, calculated according to the eqs. (1) and (2) in the Supporting Information. These experimental results indicated that the FdU-PCL conjugates could self-assemble into stable micelles with the NO precursor PSF loaded. The stability of the Micelles was evaluated, the results of which are shown in Fig. 3. The average diameter and PDI of the Micelles in either PBS buffer or fetal bovine serum (FBS) under physiological conditions (pH 7.4, 37 °C) changed little during the period of 72 h, indicative of the high stability

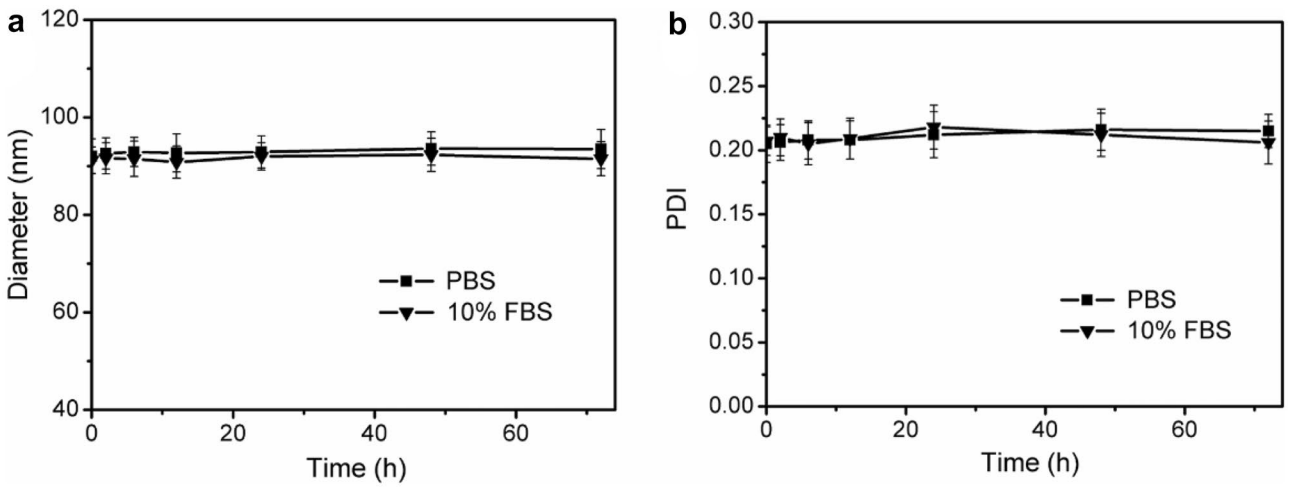

Fig. 3 Changes of average diameter (**a**) and polydispersity index (PDI) (**b**) of the Micelles in PBS buffer or 10% FBS solution (pH 7.4, 37 °C) during 72 h. The data are presented as average ± standard deviation ($n = 3$)

of the Micelles in physiological environment outside cancer cells. This would avoid undesired drug release before the Micelles arrived at target sites.

Drug delivery properties

The drug delivery properties of the Micelles are crucial for treatment of cancer. The ester bond connecting FdU and PCL is vulnerable to acid and a lowered pH will decompose the Micelles by cleaving the ester bond. The otherwise entrapped PSF is freed, and releases NO once encountering GSH. The GSH-triggered NO release from the Micelles in PBS buffer was measured with an amperometric method. The cumulative NO released under different conditions is shown in Fig. 4a. The pH value did not affect the NO release in the absence of GSH. When 10 mM GSH existed in the buffer, NO was detected even at pH 7.4. As the pH value was reduced to 5, a significant amount of NO was released, since it was more probable for the free PSF to contact GSH. A cumulative amount of 34.5 μM NO was released at 48 h under the conditions characteristic of intracellular environment (10 mM GSH, pH 5 and 37 °C), indicating the stimuli-responsive NO delivery properties of the Micelles.

On the other hand, the release of FdU from the micelles was investigated, and the release profiles are shown in Fig. 4b. The release profile of free FdU obtained with the same method was also shown as a control. At pH 7.4, the amount of released FdU was fairly small over the 48 h period. As the pH was lowered to 6, much more FdU was released due to the decomposition of the Micelles. At an even lower pH value of 5, which is typical of endolysosomal system in cancer cells, around 60% of the FdU was released after 48 h, more than the case at pH 6, because more Micelles were decomposed under increasingly acidic

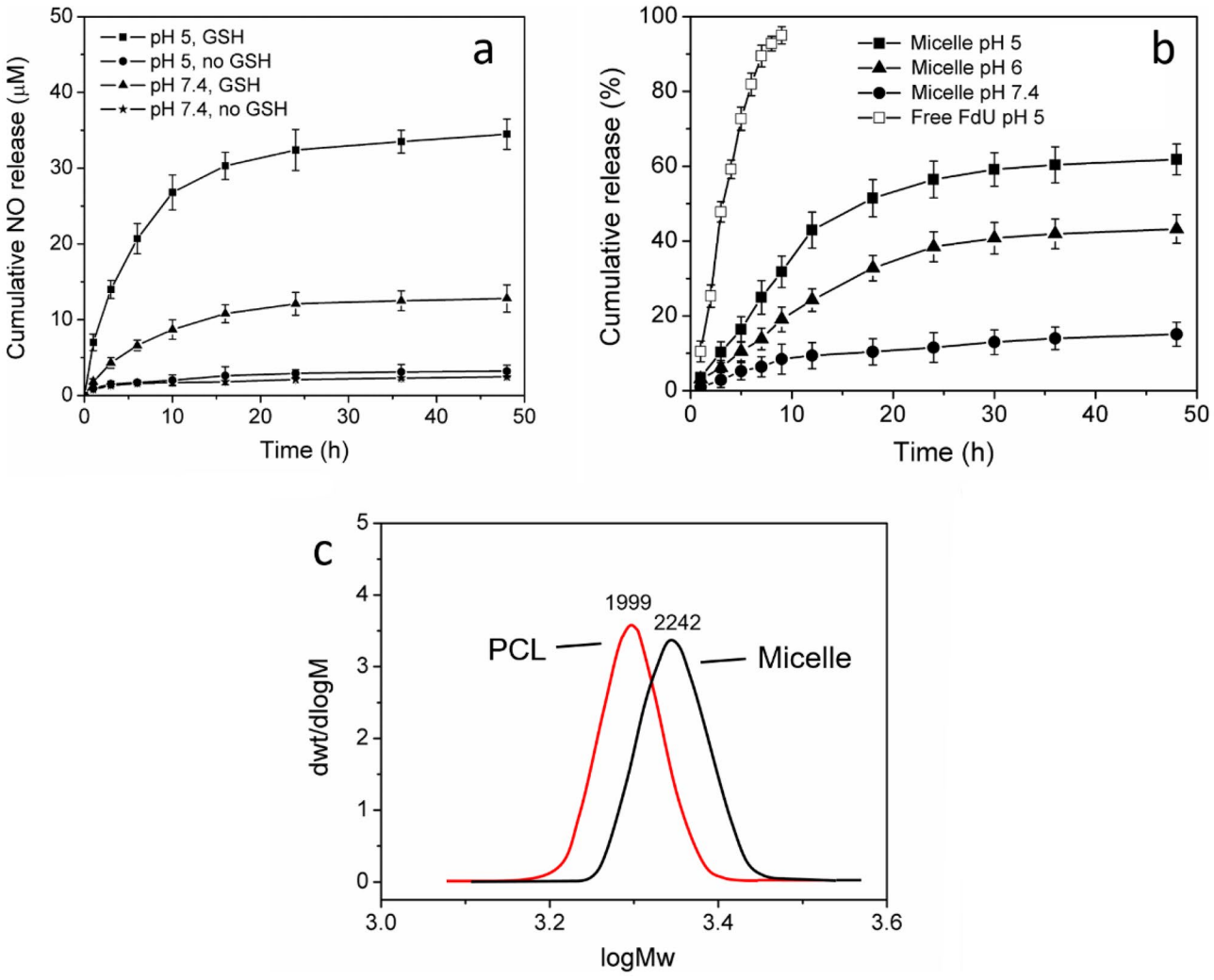

Fig. 4 In vitro release of NO (**a**) and FdU (**b**) from the Micelles under different conditions (10 mM GSH, 37 °C). (**c**) GPC traces of the Micelles (without PSF) and the decomposition product PCL at pH 5

condition. On the basis of Fig. 4, the release half-life of NO and FdU in typical intracellular environment was 4.3 h and 8.4 h, respectively. The half-lives of the two drugs are in the same order of magnitudes, which means the synergistic treatment based on FdU and NO can be readily achieved. This is imperative for a drug delivery system towards NO-assisted chemotherapy.

The decomposition of the Micelles under acidic conditions was confirmed by measuring the molecular weight of the Micelles before and after subjecting to lowered pH by GPC. The GPC traces are shown in Fig. 4c, demonstrating that the ester bond in the Micelles was broken under acidic conditions, leading to decomposition of the Micelles and the release of drugs.

Anticancer properties

Cell uptake of the Micelles and intracellular NO release were examined by cell fluorescence observation. Human Cervical Carcinoma (HeLa) cells were chosen as the representative cancer cells in this study. The nucleus of HeLa cells was stained by DAPI, a DNA-binding dye with bright blue emission, and the HeLa cells were then incubated with the Micelles for 2 h at 37 °C. Confocal laser scanning microscopy was adopted to observe the cells. Cu-2-{2-chloro-6-hydroxy-5-[(2-methyl-quinolin-8-ylamino)-methyl]-3-oxo-3H-xanthen-9-yl}-benzoic acid (CuFL) was used as a NO probe [26]. As shown in Fig. 5a, no green fluorescence characteristic of CuFL in combination with NO could be observed from the cells at 0 h. In contrast, green fluorescence was observed after 6 h incubation, indicating that NO was released from the decomposed Micelles in the cancer cells. The internalized Micelles were mainly distributed in the cytoplasm, as demonstrated by the merged fluorescence image. Another 6 h incubation resulted in stronger green fluorescence, as more NO molecules were released and accumulated in the cells with the further decomposition of the Micelles.

The anticancer effect of the Micelles on HeLa cells was assessed by MTT assay. The HeLa cells were incubated with FdU, FdU/PSF mixture, Micelles or blank micelles at different equivalent FdU concentrations for 24 h. The untreated HeLa cells were taken as a control. As shown in Fig. 5b, free FdU could inhibit the proliferation of HeLa cells, but not significantly because of the multi-drug resistance (MDR) effect [27]. The formulation of FdU/PSF mixture inhibited the cell proliferation to a larger extent than free FdU at the same equivalent FdU concentration, likely due to the reduced MDR effect in the presence of NO [28]. The blank micelles had stronger inhibitory effect on the cancer cells, taking advantage of the enhanced permeation and retention (EPR) effect of nanoparticles. In the

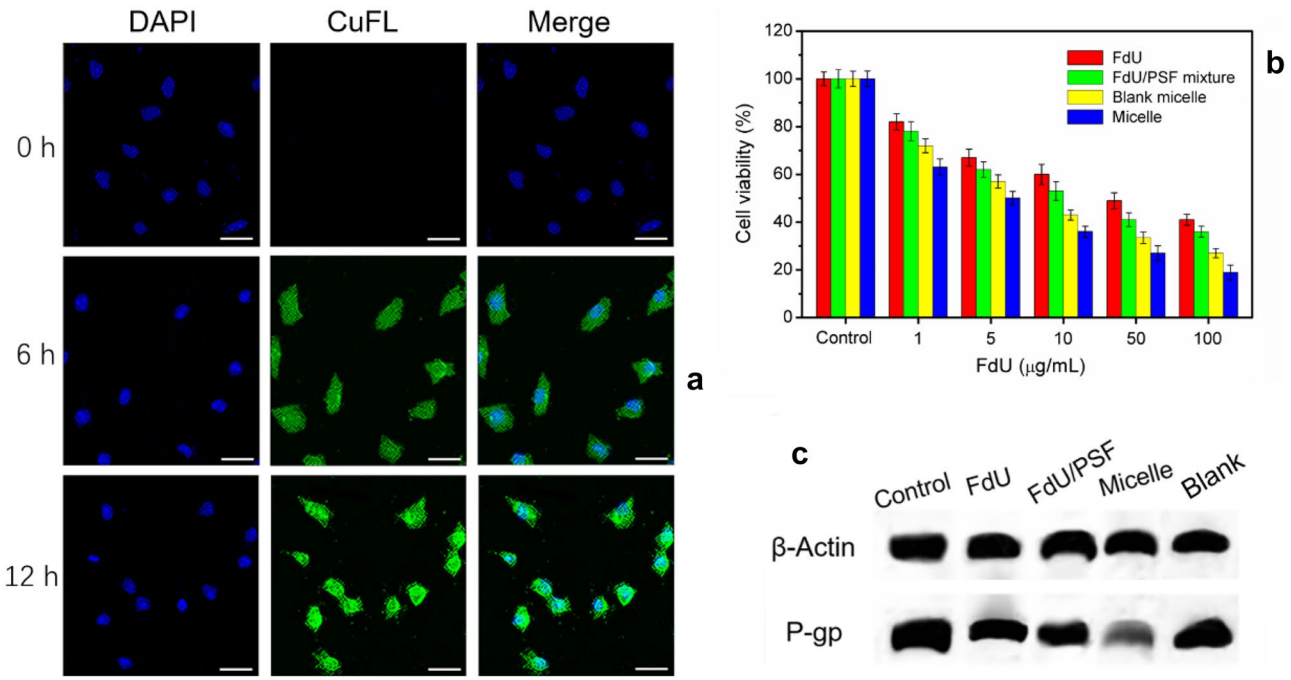

Fig. 5 (**a**) Fluorescence images of HeLa cells incubated with Micelles as well as CuFL for varied time periods at 37 °C. The scale bars represent 25 μm. (**b**) Cytotoxicity of different formulations to HeLa cells at different equivalent FdU concentrations based on MTT assay. The data are presented as average ± standard deviation ($n = 5$). (**c**) The P-gp expression in HeLa cells treated with different formulations based on Western blot. Untreated HeLa cells were used as a control, and β-actin was used as the loading control

case of the Micelles, the cell viability greatly decreased in comparison with the other formulations. Internalized by the cells, the Micelles entered the endolysosomal system, where the lowered pH triggered the decomposition of the Micelles and thus the release of FdU and PSF. The intracellular GSH gave rise to the NO release from the PSF. Compared with the FdU/PSF mixture, the drugs released from the stimuli-responsive Micelles could escape from the endolysosomal system more rapidly. Consequently, more FdU and NO could enter the nucleus to achieve higher therapeutic efficacy. NO is able to reduce or reverse the MDR effect, preventing the efflux of chemotherapeutic drugs. Also, NO of appropriate concentration may kill cancer cells [13]. The synergistic effect from FdU and NO played a critical role in cancer treatment.

The overexpression of P-glycoprotein (P-gp) is regarded as an efflux pump to expel chemotherapeutic drugs out of the cancer cells and accounts for the MDR effect to a great degree [29]. NO has been reported as being able to suppress the overexpression of P-gp. The P-gp expression of the HeLa cells was examined by Western blotting to evidence the MDR reversal ability of NO. Incubated with different drug formulations for 1 h, the P-gp expression of the cells was analyzed. As shown in Fig. 5c, the P-gp expression was not affected by free FdU and the blank micelles. The FdU/PSF mixture down-regulated the P-gp expression slightly, as reflected by the weaker band signal. In the case of the Micelles, the P-gp expression was substantially suppressed, indicating the Micelles could reduce the efflux of FdU more greatly than the FdU/PSF mixture. This was in good accordance with the MTT results and confirmed the pivotal role of NO in inhibiting cancer cells through MDR reversal.

Furthermore, in vivo animal experiments were conducted to investigate the anticancer efficacy of the Micelles.

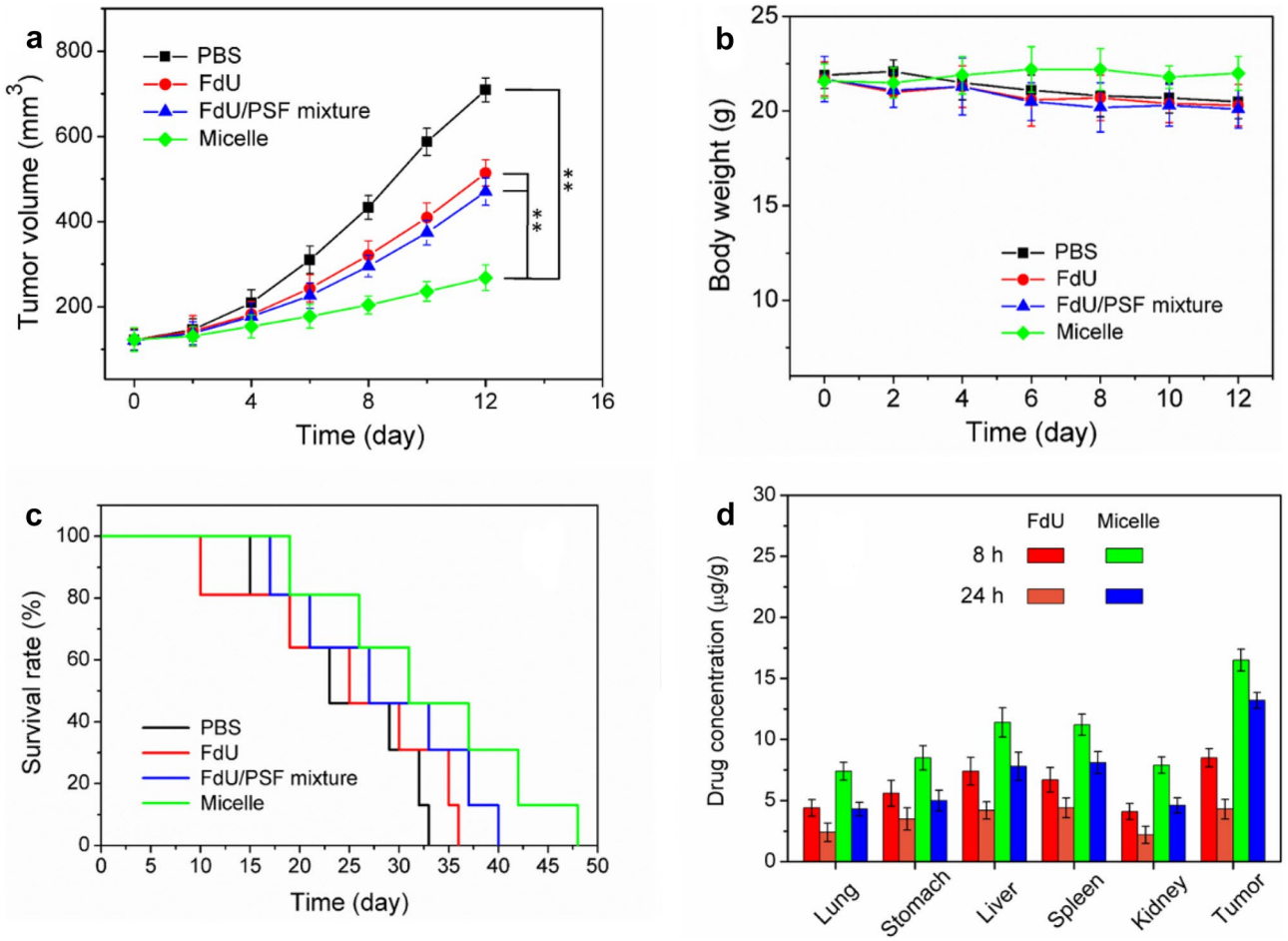

Fig. 6 (**a**) Tumor growth in the mice treated with tail vein injection of different formulations every other day over a period of 12 days. $^{**}P<0.01$. The data are presented as average ± standard deviation ($n=5$). (**b**) Body weight changes of the mice after treatment with these formulations. The data are presented as average ± standard deviation ($n=5$). (**c**) Changes of survival rate with time for the mice treated with different formulations. (**d**) Distribution of FdU and Micelles in the mice body at 8 h and 24 h after tail vein injection. The data are presented as average ± standard deviation ($n=3$)

BALB/c mice bearing an inoculated HeLa cells were injected with different drug formulations via tail vein every two days. The mice treated with PBS buffer were taken as a control. The case of Micelles was compared with the cases of FdU and FdU/PSF mixture. The tumor volume and body weight of the mice subjected to different treatments were recorded in a period of 12 days. It is indicated in Fig. 6a that the free FdU and FdU/PSF mixture inhibited the growth of HeLa tumors, as compared with the case of PBS treatment. It is clear that the mice treated with the Micelles had much stronger tumor inhibitory than the free FdU and FdU/PSF mixture. After 12 days, the tumor grew from 123 to 268 mm^3, while the tumor on the mice of control group grew from 122 to 709 mm^3 over the same period. Figure 6b shows the changes of body weight of the mice treated differently. During the 12-day period, body weight of the mice treated with the Micelles changed little, and was larger than those of the mice treated with other formulations. These results suggested that the Micelles did not have severe side effects on body.

The mortality of the treated mice was monitored during a period of 50 days, as displayed in Fig. 6c. For the control group, all the mice were dead after 33 days. The mice treated with free FdU were all dead at the 36th day. The mice treated with the FdU/PSF mixture lived for a longer period, with the survival rate decreasing to 0 at 40th day. As for the mice treated with the Micelles, the survival rate decreased to 0 at 48th day, suggesting the longer survival time of the mice. It could be concluded that the Micelles had higher therapeutic efficacy originating from the synergistic effect of FdU and NO.

Finally, we investigated the distribution of Micelles in the tumor and major organs of the tumor-bearing mice. The mice were sacrificed at 8 h and 24 h after tail vein injection of the Micelles and free FdU for comparison. At 8 h post injection, as shown in Fig. 6d, the content of free FdU in lung, stomach and kidney was similar, and the tumor had similar FdU content to liver and spleen. At 24 h post injection, the FdU content in all the parts decreased a lot, as the FdU was metabolized. The content of Micelles in all the parts was higher than the content of FdU at the same time points, indicating that the blood clearance of Micelles was less than that of the free FdU. The Micelles were distributed in the tumor much more than in the major organs, suggesting the higher accumulation of the Micelles in the tumor. It is also noted that the decrease in the content of Micelles in the tumor was less than that in the organs, indicative of longer retention of the Micelles inside the tumor. The high accumulation and long retention favor the enhancement of therapeutic efficacy.

Based on the in vitro cell assay and in vivo animal experiments, we found that the Micelles were able to release both FdU and NO in response of lowered pH and intracellular GSH. The FdU inhibits the growth of cancer cells, while the NO reduces the MDR effect to enhance the chemotherapeutic efficacy of FdU. Therefore, synergistic therapeutic effect can be realized by using the Micelles as the drug delivery system.

Conclusions

To conclude, the FdU-PCL conjugates were designed, synthesized and self-assembled together with PSF to form Micelles as drug delivery platforms. The Micelles had an average diameter of ~ 90 nm and a narrow size distribution, and could keep stable in physiological environment. Under acidic conditions, the Micelles would decompose and release the chemotherapeutic drug FdU and the NO precursor PSF. Release of NO from the PSF could be triggered by GSH, and co-delivery of FdU and NO was thus achieved. In vitro cell assay demonstrated that the Micelles released FdU and NO in response to intracellular pH and GSH. The NO suppressed the expression of P-gp and thus reduced the MDR effect to enhance the chemotherapeutic efficacy. The results of in vivo experiments confirmed the synergistic anticancer effect of FdU and NO released from the Micelles. The rationally designed dual drug-loading Micelles displayed great potential as a therapeutic system. This study offers new insights into synergistic cancer therapy.

Supplementary information The online version contains supplementary material available at https://doi.org/10.1007/s10965-021-02645-4.

References

1. Li C, Shen J, Yang J, Yan J, Yu H, Liu J (2018) NIR-triggered release of nitric oxide with upconversion nanoparticles inhibits platelet aggregation in blood samples. Part Part Syst Charact 35:1700281
2. Burnett AL, Lowenstein CJ, Bredt DS, Chang T, Snyder SH (1992) Nitric oxide: a physiologic mediator of penile erection. Science 257:401–403
3. Keefer LK (2005) Nitric oxide (NO)-and nitroxyl (HNO)-generating diazeniumdiolates (NONOates): emerging commercial opportunities. Curr Top Med Chem 5:625–636
4. Kushima H, Mori Y, Koshibu M, Hiromura M, Kohashi K, Terasaki M et al (2017) The role of endothelial nitric oxide in the anti-restenotic effects of liraglutide in a mouse model of restenosis. Cardiovasc Diabetol 16:122
5. Fang FC (1997) Perspectives series: host/pathogen interactions. Mechanisms of nitric oxide-related antimicrobial activity. J Clin Invest 99:2818–2825
6. Ying L, Hofseth LJ (2007) An emerging role for endothelial nitric oxide synthase in chronic inflammation and cancer. Cancer Res 67:1407–1410
7. Walford G, Loscalzo J (2003) Nitric oxide in vascular biology. J Thromb 1:2112–2118
8. Luo JD, Chen AF (2005) Nitric oxide: a newly discovered function on wound healing. Acta Pharmacol Sin 26:259–264

9. Ying L, Hofseth LJ (1994) Inhibition of nitric oxide synthesis suppresses sleep in rabbits. Am J Physiol 266:R151–R157
10. Song Q, Tan S, Zhuang X, Guo Y, Zhao Y, Wu T et al (2014) Nitric oxide releasing D-α-tocopheryl polyethylene glycol succinate for enhancing antitumor activity of doxorubicin. Mol Pharmaceutics 11:4118–4129
11. Carpenter AW, Schoenfisch MH (2012) Nitric oxide release: Part II Therapeutic applications. Chem Soc Rev 41:3742–3752
12. Huang Z, Fu J, Zhang Y (2017) Nitric oxide donor-based cancer therapy: Advances and prospects. J Med Chem 60:7617–7635
13. Zhang X, Tian G, Yin W, Wang L, Zheng X, Yan L et al (2015) Controllable generation of nitric oxide by near-infrared-sensitized upconversion nanoparticles for tumor therapy. Adv Funct Mater 25:3049–3056
14. Chung MF, Liu HY, Lin KJ, Chia WT, Sung HW (2015) A pH-responsive carrier system that generates NO bubbles to trigger drug release and reverse P-glycoprotein-mediated multidrug resistance. Angew Chem Int Ed 54:9890–9893
15. Tan L, He C, Chu X, Chu Y, Ding Y (2020) Charge-reversal ZnO-based nanospheres for stimuli-responsive release of multiple agents towards synergistic cancer therapy. Chem Eng J 395:125177
16. Niu X, Cao J, Zhang Y, Gao X, Cheng M, Liu Y et al (2019) A glutathione responsive nitric oxide release system based on charge-reversal chitosan nanoparticles for enhancing synergistic effect against multidrug resistance tumor. Nanomedicine 20:102015
17. Tan L, Wan A, Li H, Lu Q (2012) Nitric oxide (NO)- and nitroxyl (HNO)-generating diazeniumdiolates (NONOates): emerging commercial opportunities. Acta Biomater 8:3744–3753
18. Ghosh S, Roy P, Prasad S, Mugesh G (2019) Crystal-facet-dependent denitrosylation: modulation of NO release from S-nitrosothiols by Cu_2O polymorphs. Chem Sci 10:5308–5318
19. Minamiyama Y, Takemura S, Imaoka S, Funae Y, Okada S et al (2007) Cytochrome P450 is responsible for nitric oxide generation from NO-aspirin and other organic nitrates. Drug Metab Pharmacokinet 22:15–19
20. Duan W, Li J, Inks ES, Chou CJ, Jia Y, Chu X et al (2015) Design, synthesis, and antitumor evaluation of novel histone deacetylase inhibitors equipped with a phenylsulfonylfuroxan module as a nitric oxide donor. J Med Chem 58:4325–4338
21. Jhaveri AM, Torchilin VP (2014) Multifunctional polymeric micelles for delivery of drugs and siRNA. Front Pharmacol 5:77
22. Mao J, Li Y, Wu T, Yuan C, Zeng B, Xu Y et al (2016) A simple dual-pH responsive prodrug-based polymeric micelles for drug delivery. ACS Appl Mater Interfaces 8:17109–17117
23. Liu C, Yuan J, Luo X, Chen M, Chen Z, Zhao Y et al (2014) Folate-decorated and Reduction-sensitive micelles assembled from amphiphilic polymer–Camptothecin conjugates for intracellular drug delivery. Mol Pharmaceutics 11:4258–4269
24. Shi J, Liu S, Yu Y, He C, Tan L, Shen Y-M (2019) RGD peptide-decorated micelles assembled from polymer–paclitaxel conjugates towards gastric cancer therapy. Colloid Surf B 180:58–67
25. Lv S, Tang Z, Zhang D, Song W, Li M, Lin J et al (2014) Well-defined polymer-drug conjugate engineered with redox and pH-sensitive release mechanism for efficient delivery of paclitaxel. J Control Release 194:220–227
26. Wong KK, Ng A, Chen XY, Ng YH, Leung YH, Ho KH et al (2012) Effect of ZnO nanoparticle properties on dye-sensitized solar cell performance. ACS Appl Mater Interfaces 4:1254–1261
27. Dai L, Li X, Duan X, Li M, Niu P, Xu H et al (2019) Anticancer efficacy of a nitric oxide-modified derivative of bifendate against multidrug-resistant cancer cells. Adv Sci 6:1801807
28. Ren Z, Gu X, Lu B, Chen Y, Chen G, Feng J et al (2016) Anticancer efficacy of a nitric oxide-modified derivative of bifendate against multidrug-resistant cancer cells. Cell Mol Med 20:1095–1105
29. Tian G, Zhang X, Zheng X, Yin W, Ruan L, Liu X et al (2014) Multifunctional RbxWO3 nanorods for simultaneous combined chemo-photothermal therapy and photoacoustic/CT imaging. Small 10:4160–4170